Two-Dimensional van der Waals Materials with Aligned In-Plane Polarization and Large Piezoelectric Effect for Self-Powered Piezoelectric Sensors

Mingjin Dai,[†,§] Zhiguo Wang,[&] Fakun Wang,[⊥] Yunfeng Qiu,[§] Jia Zhang,[§] Cheng-Yan Xu,[†,§] Tianyou Zhai,[⊥] Wenwu Cao,[‡] Yongqing Fu,[$] Dechang Jia,[†] Yu Zhou,[†] Ping-An Hu*[,†,§]

[†]School of Materials Science and Engineering, Harbin Institute of Technology, Harbin 150001, China

[§]MOE Key Laboratory of Micro-Systems and Micro-Structures Manufacturing, Harbin Institute of Technology, Harbin 150001, China

[&]School of Electronics Science and Engineering, University of Electronic Science and Technology of China, Chengdu 610054, China

[⊥]State Key Laboratory of Material Processing and Die and Mould Technology, School of Materials Science and Engineering, Huazhong University of Science and Technology, Wuhan 430074, P. R. China

[‡]Department of Mathematics and Materials Research Institute, The Pennsylvania State University, University Park, Pennsylvania 16802, United States

[$]Faculty of Engineering & Environment, Northumbria University, Newcastle upon Tyne, NE1 8ST, UK.

Supporting Information Placeholder

ABSTRACT: Piezoelectric two-dimensional (2D) van der Waals (vdWs) materials are highly desirable for applications in miniaturized and flexible/wearable devices. However, the reverse-polarization between adjacent layers in current 2D layered materials results in decreasing their in-plane piezoelectric coefficients with layer number, which limits their practical applications. Here, we report a class of 2D layered materials with an identical orientation of in-plane polarization. Their piezoelectric coefficients (e_{22}) increase with layer number, thereby allowing for the fabrication of flexible piezotronic devices with large piezoelectric responsivity and excellent mechanical durability. The piezoelectric outputs can reach up to 0.363 V for a 7-layer α-In_2Se_3 device, with a current responsivity of 598.1 pA for 1% strain, which is one order of magnitude higher than the values of the reported 2D piezoelectrics. The self-powered piezoelectric sensors made of these newly developed 2D layered materials have been successfully used for real-time health monitoring, proving their suitability for the fabrication of flexible piezotronic devices due to their large piezoelectric responses and excellent mechanical durability.

KEYWORDS: indium selenide, asymmetric structure, stacking sequence, robust piezoelectricity, piezoresponsivity, sensors

INTRODUCTION

Piezoelectric materials with intrinsic non-centrosymmetric crystal structures allow for interconversion between electrical energy and mechanical energy.[1] They are widely used for actuators, energy harvesters, functional sensors, and other applications.[2-4] Since the first demonstration of piezoelectricity in quartz crystals in 1880 by the brothers Pierre Curie and Jacques Curie, a series of piezoelectric materials were developed, including piezoelectric crystals (such as quartz, GaN, $BaTiO_3$, etc.) and piezoelectric ceramics (such as lead zirconate titanate (PZT) system). Among these piezoelectric materials, piezoelectric ceramics such as PZT and barium titanate (BTO) are the most widely used due to their excellent electromechanical conversion.[5]

For some important applications, piezoelectric materials are required to be thin, flexible, chemically stable and also bio-compatible such as artificial

intelligent interface electronics, flexible/wearable devices, and bio-implantable electronics.[4] These requirements are difficult to be achieved using the conventional piezoelectric ceramics, because they have no mechanical flexibility and lack chemical stability in bio-environment; and some of them contain toxic components.[6] These problems may be solved by the use of strong, flexible, ultrathin piezoelectrics of 2D layered materials. Since the pioneering studies of piezoelectricity in monolayer MoS_2 by the research groups of Wang and Zhang in 2014, researchers focused on improving the piezoelectric efficiency of the 2D materials.[7,8] So far, the reported piezoelectric vdWs layered semiconductors include hexagonal boron nitride (*h*-BN), transition metal dichalcogenides (TMDs), layer-phase group III monochalcogenides (i.e. GaS, GaSe, and InSe), and group IV monochalcogenides (MX, M=Sn or Ge, X=Se or S).[9-13] These layered materials have an inversion symmetry in their bulk structures, whereas they lose the inversion symmetry as their thickness is thinned down to monolayer or a few odd-layers.[7,8] Furthermore, their in-plane piezoelectricity is significantly decreased with the increase of atomic layer number, because the reversed polarization directions between adjacent layers result in the cancellation of polarization. Therefore, the monolayer structure has the largest in-plane piezoelectric coefficient for those vdWs layered materials, even larger than some conventional bulk piezoelectric crystals, such as gallium nitride and aluminum nitride.[9]

However, there are two bottleneck problems for applying atomically thin monolayer piezoelectrics in practical device applications: (i) Their small piezoelectric outputs cannot produce high responsivity due to its exceedingly small effective volume. For example, the piezoelectric current and voltage outputs are only about dozens of pA and mV for monolayer MoS_2, respectively.[7] (ii) The poor mechanical stability for the monolayer cannot sustain long-term durability.[14-16] To address above problems, a turbostratic stacking approach was demonstrated to manipulate the polarization in artificial bilayer or multilayers for inducing or enhancing the degree of structural non-centrosymmetry.[14] However, this complex process and the uncontrollable performance of the artificial multilayer hinder its potential for broad practical applications. Herein, a new class of 2D piezoelectric materials is proposed that exhibit the same polarization orientation between adjacent monolayers, which can simultaneously offer large piezoelectric output signals and long-term durability by use of multilayer structures.

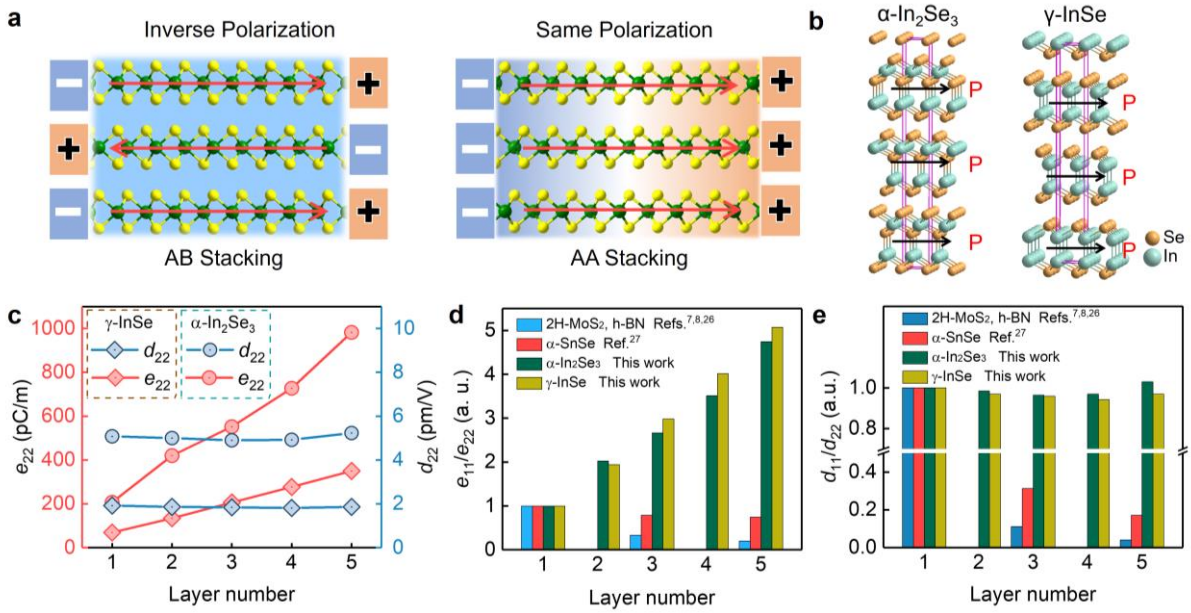

Figure 1. Piezoelectricity in vdWs layered materials. (a) The distribution of in-plane polarization under tensile strain in vdWs layered materials. The polarized direction (red arrows) are inverse or same in AB or AA stacking case. (b) Piezoelectric with same polarization direction (black arrows) in a unit cell of α-In_2Se_3 (left) and γ-InSe (right). (c) Layer number dependence of piezoelectric stress coefficients (e_{22}) and piezoelectric strain coefficients (d_{22}) for few-layer α-In_2Se_3 and γ-InSe. (d, e) Comparison of piezoelectric coefficients dependence on layer number with other typical two-dimensional materials. (The theoretical data (e_{11}/e_{22} and d_{11}/d_{22}) for *h*-BN, 2H-MoS_2 and SnSe are adopted from refs.[7,8,26,27]).

RESULTS AND DISCUSSION

Stacking sequence governed piezoelectricity in 2D vdWs materials. Firstly, we discuss the relationship between crystal structure and piezoelectricity for these materials. The vdWs layered semiconductors have rich polytype phases with diverse physical properties in different stacking configurations and possess different crystal symmetries.[17,18] For example, semiconducting MoS_2, as a most studied vdWs layered material, can be in either 2H-type or 3R-type structures when they are in AB or AA stacking configurations, corresponding to centrosymmetric and non-centrosymmetric crystal structures, respectively.[19] The 2H-MoS_2 with the AB stacking sequence is the most thermodynamically stable phase, which can be produced with a large yield.[20] For the 2H-MoS_2 with the AB stacking, the strain induced dipoles have reverse directions in adjacent layers, and the piezoelectric contribution of each layer is neutralized by its neighboring layer. As a result, the overall piezoelectric effect is only significant for a few odd numbers of monolayers (left in Figure 1a). In contrast, the 3R-MoS_2 layers with the AA stacking have identical directions of strain induced dipoles in adjacent layers, thus resulting in strong piezoelectric effect in multilayer structures (right in Figure 1a). However, the thermodynamic instability and uncontrollability of synthesis make 3R-MoS_2 an unsuitable candidate for the 2D piezoelectric material.[17] Indium selenides, on the other hand, belong to a complex family of polytypes with different stoichiometric ratios and phases, such as layered In_2Se_3 (α and β phase) and InSe (β, γ and ε phase). The indium selenides in multilayers or bulk crystal are thermodynamically stable in ambient conditions, and can be produced in a pure phase by a suitable procedure, such as chemical vapor deposition (CVD), vapor transport, Bridgeman method and so on.[21] Both α-In_2Se_3 and γ-InSe have non-centrosymmetric crystal structures, corresponding to *R3m* (No.160) space group. Recently, studies of ferroelectricity in the α-In_2Se_3 proved that it was a promising new vdWs layered material for potential piezoelectric applications.[22-25]

In the structures of α-In_2Se_3 and γ-InSe (Figure 1b), there are three layers stacked vertically via vdWs interaction with AA sequence in a unit cell (indicated by pink frame in Figure 1b). This stable stacking configuration leads to the same in-plane polarized directions in all the layers under a uniaxial strain (more details in Supporting Information). Hence, their multilayer structures should always exhibit piezoelectric effects no matter the existence of odd- or even-layer number, and should have much higher polarized charge densities than those of the currently reported 2D piezoelectric materials that have inversion centers in their even-layer flakes.

To verify these assumptions, the piezoelectric coefficients of both α-In_2Se_3 and γ-InSe as a function of layer number were obtained through the first-principles simulations using density functional theory (DFT). The obtained planar elastic stiffness coefficients C_{11} and C_{12}, relaxed-ion piezoelectric stress coefficients e_{22}, and relaxed-ion strain coefficients d_{22}, are listed in Tables S1 and S2. The value of piezoelectric stress coefficient e_{22}, is proportional to layer numbers, varying from 207 pC/m for 1L to 982 pC/m for 5L (Figure 1c). Thus, the piezoelectric strain coefficients d_{22} remains at a value of 5.022±0.21 pm/V inα-In_2Se_3 when the layer number is increased from one layer (1L) to five layer (5L). As for γ-InSe, its e_{22} value is increased from 69 to 350 pC/m (for 1L to 5L), and its d_{22} remains a value of 1.86±0.06 pm/V. Clearly, the piezoelectricity in both α-In_2Se_3 and γ-InSe shows a strong dependence on layer number (Figure 1d and e), which is totally different from those of the currently reported piezoelectric layered materials, such as 2H-MoS_2, *h*-BN and α-SnSe.[7,8,26,27] The calculated piezoelectric coefficients e_{11} and d_{11} of 2H-MoS_2, *h*-BN and α-SnSe are decreased with odd layers from 1L, 3L, to 5L, and disappear with even layers of 2L and 4L. Whereas the d_{22} values of multilayer α-In_2Se_3 and γ-InSe remain a constant value despite of its odd- or even-layer number, and their e_{22} value is increased as layer number is increased from 1L to 5L (Figure 1d and 1e).

Characterization and layer number dependent piezoelectricity in α-In_2Se_3. The piezoelectric properties of 2D α-In_2Se_3 were experimentally investigated. The monolayer and few-layer α-In_2Se_3 flakes (up to 7L) were grown using a CVD method (Figure S6, Supporting Information). High-resolution transmission electron microscope, selected area electron diffraction and atomic force microscopy were utilized to confirm the high crystalline quality and the thickness of as-prepared α-In_2Se_3 (Figure S7 and S8, Supporting Information). Three Raman peaks at 104, 183 and 202 cm^{-1} were attributed to A_1(LO+TO), A_1(LO) and A_1(LO) vibration modes, respectively (Figure 2a), indicating the lack of an inversion symmetry in α-In_2Se_3 with *R3m* space group.[24] Further, second harmonics generation (SHG) was utilized to determine the symmetry variations in a few-layer α-In_2Se_3.[28] To demonstrate the retaining of broken inversion symmetry for the α-In_2Se_3 with both odd- and even-layers, the SHG intensity mappings were taken in both parallel and perpendicular polarization configurations from the samples with different layer numbers (e.g., 3L and 5L). The SHG intensity for the 5L α-In_2Se_3 flake was higher than that of 3L flake (Figure S10, Supporting Information). This indicates that there is indeed no inversion center for the even-layer α-In_2Se_3, and each layer exhibits the same In-Se bond direction in the adjacent layers.[29] Moreover, the SHG intensity mapping shows a uniform intensity distribution over the

entire area, indicating a high crystalline quality of the as-grown α-In_2Se_3 flake (Figure 2b). Furthermore, the angle dependence of SHG intensity taken in parallel polarization configurations shows a six-fold rotational symmetry ($I = I_0 \cos^2(3\theta)$), which also validates that the α-In_2Se_3 belongs to *R3m* space group with a three-fold rotational symmetry (Figure 2c and Figure S10d in Supporting Information).[17] This broken center symmetry in rational thickness is of the essence for the unusual piezoelectricity in multilayer α-In_2Se_3.[24]

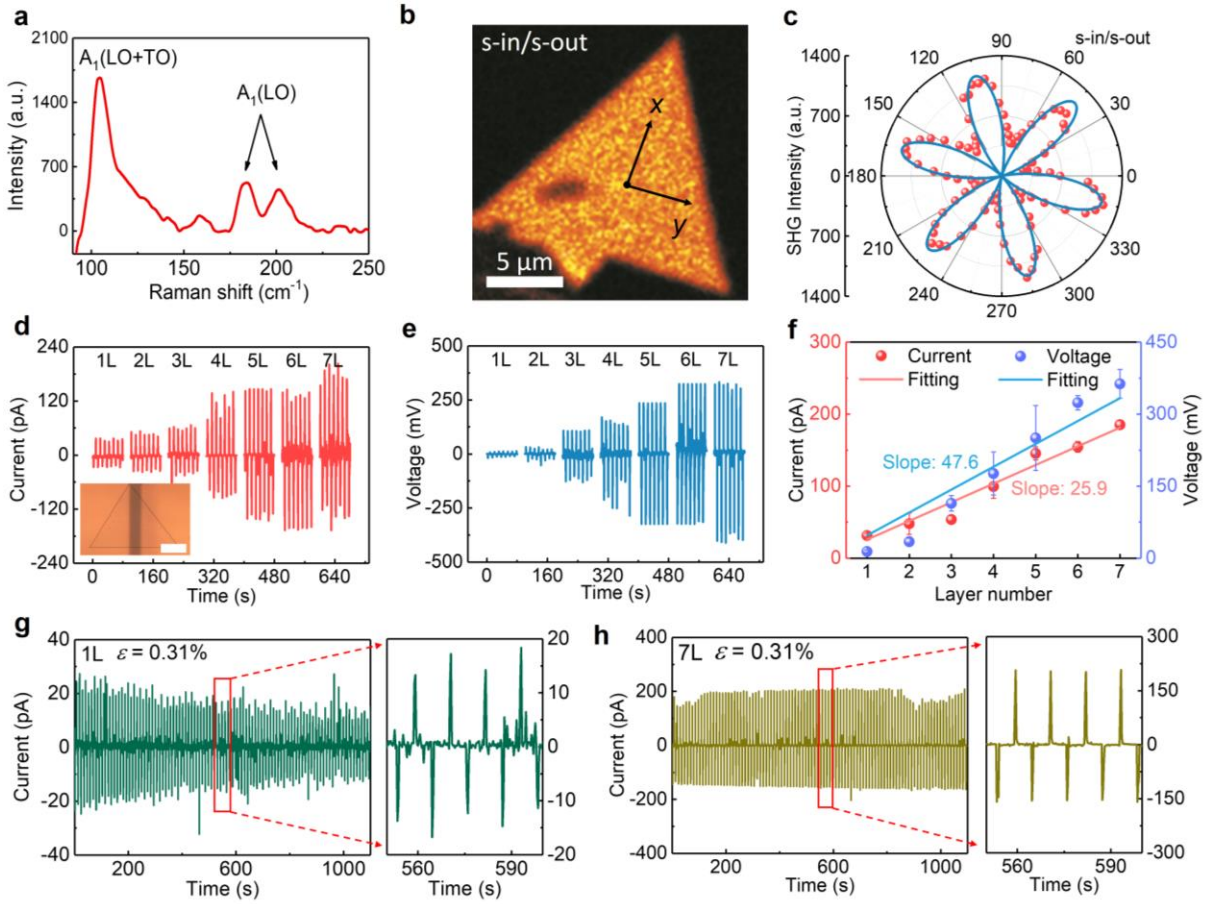

Figure 2. Structure and piezoelectricity of as-synthesized α-In_2Se_3. (a) Raman spectra of α-In_2Se_3 transferred onto SiO_2/Si substrate. (b) SHG mapping of a single α-In_2Se_3 crystal on mica. (c) The polarization angle θ dependent SHG intensity. It exhibits a clear six-fold rotational symmetry ($I = I_0 \cos^2(3\theta)$). (d) Current responses in α-In_2Se_3 devices with different layers (from 1L to 7L) under periodic strain. Inset: a typical optical image of α-In_2Se_3 based device. Scale bar: 10 μm. (e) Voltage responses in α-In_2Se_3 devices with different layers (from 1L to 7L) under periodic strain. (f) The piezoelectric current and voltage outputs as a function of α-In_2Se_3 layer number. (g, h) Stability of α-In_2Se_3 piezoelectric device. Current response from cycling test a 1L α-In_2Se_3 device (g) and a 7L α-In_2Se_3 device (h). The piezoelectric device based on 7L α-In_2Se_3 shows better durability than that of 1L α-In_2Se_3. The current and voltage outputs shown in Figure 2d-h were obtained under a fixed strain of 0.31% with a strain velocity of 10 mm/s.

To measure the piezoelectric properties, two-terminal devices with a channel length of 5 μm and a width of 60 μm were fabricated using α-In_2Se_3 flakes with different thicknesses (from 1L to 7L) (Figure S11, Supporting Information). Considering the degradation of indium selenide flakes in ambient conditions, all devices were packed by polydimethylsiloxane (PDMS) thin film (see Method in Supporting Information).[30] The piezoelectric responses of the devices (including current and voltage outputs) were systematically studied (the detailed data is provided in Supporting Information). The intrinsic piezoelectricity of α-In_2Se_3 flakes was confirmed by monolayer device.[7,31] More importantly, we investigated the layer number influence on the piezoelectric properties of α-In_2Se_3 flakes. Here, all the output results were obtained with a fixed applied strain (0.31%) and strain velocity (10 mm/s), and a device size of 5×60 μm^2. The recorded output peak currents and voltages are increased from 31.5±3.0 to 185.4±6.0 pA and from 14.0±3.0 to 363.3±30.0 mV with the increase of layer number from

1L to 7L (Figure 2d and 2e). Figure 2f shows the output performance of the α-In_2Se_3 device as a function of layer number (from 1L to 7L). The output currents and voltages are increased almost linearly with the increase of layer number, which originates from the addition of contact area with a constant polarized charge density. The relationship between the output peak current (I_p) and layer number (n) can be represented as: $I_p \propto n$ (the detailed analysis is provided in Supporting Information). This makes it more sensitive to strain change than other 2D layered piezoelectric materials reported in the literature (see Table S4, Supporting Information). For example, the current responsivity of 7L α-In_2Se_3 can reach up to around 598.1±19.4 pA for each 1% stain, which is about one order of magnitude higher than that of monolayer 2H-MoS_2 (55.1±12.3 pA).[7]

Moreover, the mechanical durability and stability of devices during strain cycling were evaluated by testing 1L and 7L α-In_2Se_3 devices (Figure 2g and 2h). After cycling over 1000 seconds, the output peak current of 1L α-In_2Se_3 device was decreased from 21.8 to 12.3 pA, which is ~ 56.4 % of the initial value, whereas the 7L α-In_2Se_3 device remained a peak current of 185.4 ±18.5 pA. In addition, the output peak voltage of the 7L α-In_2Se_3 device remains a constant without apparent decreases (Figure S19, Supporting Information). The good mechanical stability and large piezoelectric response endow the multilayer structure to be suitable for practical applications in flexible/wearable electronics and implant devices.

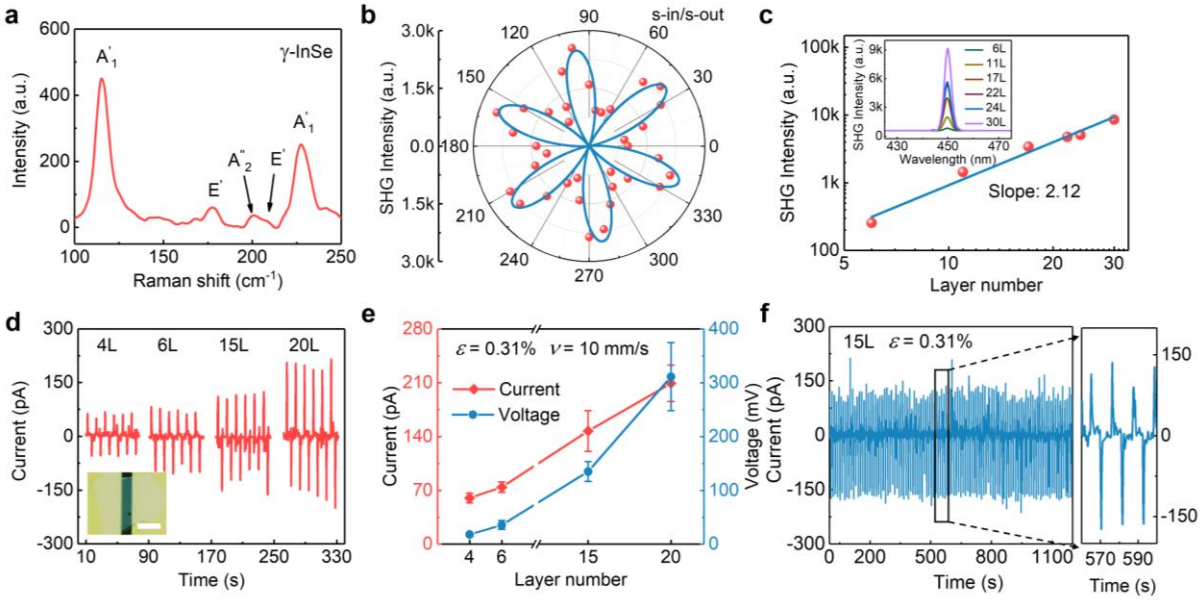

Figure 3. Structure and piezoelectricity of exfoliated γ-InSe. (a) Raman spectra of γ-InSe. (b) The polarization angle (θ) dependent SHG intensity of γ-InSe. It exhibits a clear six-fold rotational symmetry ($I = I_0 \cos^2(3\theta)$). (c) SHG Intensity as a function of γ-InSe layer number. Inset: the SHG intensity of γ-InSe with different layer numbers. (d) Current responses in γ-InSe devices with different layers under periodic strain of 0.31% with a strain velocity of 10 mm/s. Inset: a typical optical image of γ-InSe based device. Scale bar: 10 μm. (e) The piezoelectric current and voltage outputs as a function of γ-InSe layer number. (f) Current response from cyclic testing a 15L γ-InSe device under a strain of 0.31% and a strain velocity of 10 mm/s.

Characterization and layer number dependent piezoelectricity in γ-InSe. In addition, we studied the structures and piezoelectricity of the exfoliated γ-InSe nanosheets. The γ-InSe has the same atomic arrangement in a monolayer with those of β- and ε-type, but has three layers stacked in a unit cell with the AA stacking sequence, which possesses a non-centrosymmetric crystal structure.[32-34] Raman spectroscopy was used to identify the structure of γ-InSe (Figure 3a). Five Raman peaks at 116 cm^{-1}, 177 cm^{-1}, 200 cm^{-1}, 208 cm^{-1} and 227 cm^{-1} are attributed to A'_1, E', A''_2, E'' and A'_1 Raman modes of γ-InSe, respectively.[34] Moreover, HRTEM and SAED pattern further confirmed the crystal structure and crystalline quality of γ-InSe flake (Figure S20, Supporting Information). The angle dependence of SHG intensity indicates a three-fold rotational symmetry of γ-InSe, which belongs to *R3m* space group (Figure 3b). Furthermore, the SHG intensity increases with the

thickness of γ-InSe, which can be well interpreted by using the equation $I \propto d^2$ (d is the layer thickness) (Figure 3c). This indicates that γ-InSe maintains a non-centrosymmetric structure for both odd- and even-layers.[35] Under the uniaxial strain, the apparent polarization is enhanced with the increase of layer numbers due to their same polarization orientations in all layers.

To further explore the piezoelectricity of multilayer γ-InSe, its piezoelectric outputs were measured along the armchair direction, and then normalized with the active area of device. The piezoelectric responses were observed in both odd- and even-layer γ-InSe devices (Figure 3d and Figure S21, Supporting Information). The current output peaks are increased from 60.0±6.4 for 4L to 209.0±23.6 pA for 20L, and the voltage output peaks are increased from 17.9±3.2 for 4L to 311.4±63.4 mV for 20L (Figure 3e). By increasing the applied strain from 0.21% to 0.62%, the current and voltage responses for the 4L γ-InSe device were increased from 19.0±5.3 to 61.5±3.5 pA and from 30.8±5.2 to 68.2±9.2 mV, respectively (Figure S22, Supporting Information). The mechanical durability and stability of a 15L γ-InSe device were further estimated using the cycling test for over 1000 seconds (Figure 3f and Figure S23, Supporting Information). There are no apparent deterioration of the current and voltage responses of this multilayer γ-InSe, indicating a promising potential for the flexible devices.

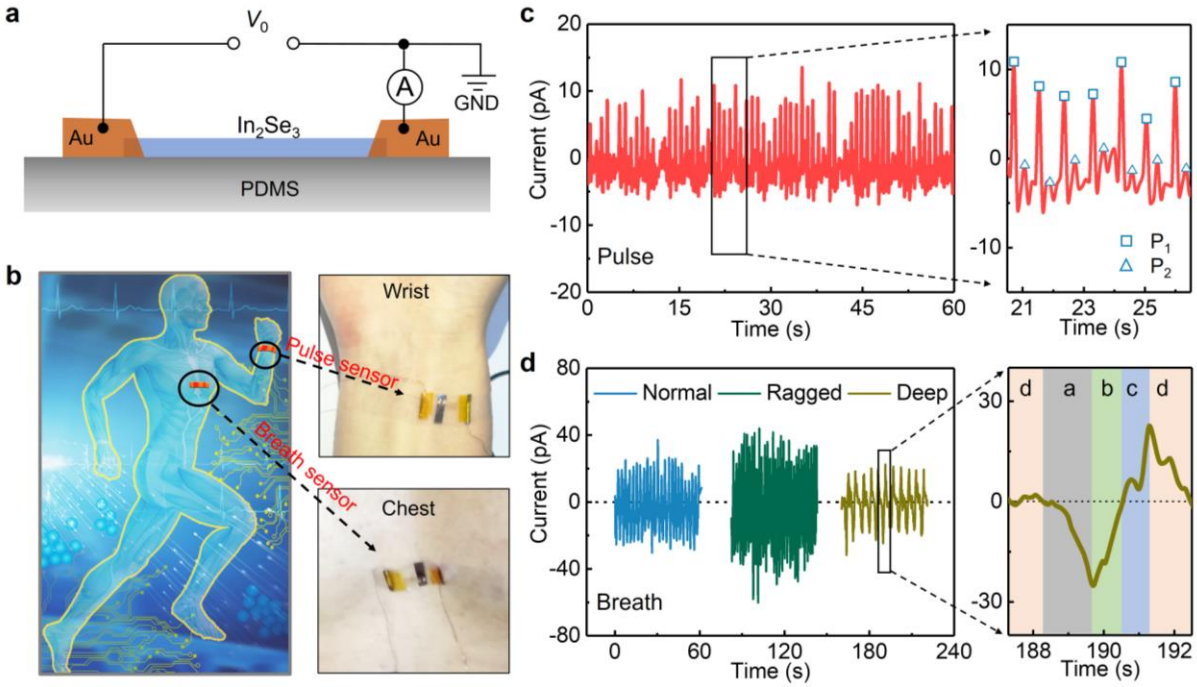

Figure 4. Self-powered piezoelectric sensors. (a) The schematic of self-powered piezotronic sensor based on a multilayer α-In_2Se_3 flake. (b) Real-time monitoring of physiological signals (left). The piezotronic sensor based on few-layer In_2Se_3 are attached on skin at wrist (top right) and chest (bottom right) for monitoring arterial pulse and breath, respectively. (c) Real-time monitoring of arterial pulse signals. Left: the measured transient arterial pulse signals. Right: the signals zoomed in black rectangle shown in left (P_1: square symbols, P_2: triangle symbols). (d) Real-time monitoring of breath signals. Left: output current responses obtained when measuring breath signals with different physical states, as indicated. Right: the time synchronization of current tracks to deep breath. (a: breath in, b: breath gap, c: breath out, d: breath gap).

Performance of the piezoelectric sensors for healthcare monitoring. The large piezoelectric responses and long-term mechanical durability of multilayer α-In_2Se_3 and γ-InSe allow us to develop sensitive and efficient flexible piezotronic sensors, such as pulse and breath monitoring.[36] Here, we demonstrate a self-powered sensor (without any external bias) using a multilayer α-In_2Se_3 flake on the soft substrate of PDMS thin films (Figure 4a). The as-made flexible and wearable sensors were utilized to perform real-time monitoring of human's pulse and breath by attaching the devices onto the wrist and chest (Figure 4b). By using our piezoelectric sensor, the pulse rate was measured to be about 72 bpm, which is consistent with the results from a commercial pulse sensor (the data were obtained from an app in a smart phone with a heart rate sensor, see Figure 4c and

Figure S24, Supporting Information). As shown in right of Figure 4c, two clear peaks are distinguishable in a pulse, which are caused by superposition of the incoming blood wave ejected by the left ventricular (P_1) and the reflected wave from the lower body (P_2).[29] Apparently, the self-powered piezoelectric multilayer device exhibits a high sensitivity and good reliability. In contrast, signals obtained from a monolayer α-In_2Se_3 device are too weak to be distinguished from the background noise (Figure S25, Supporting Information). Moreover, the multilayer α-In_2Se_3 device also shows a good performance in monitoring breath (Figure 4d). Three different breath states can be accurately recorded. With regard to ragged breathing (e.g., the breath frequency is much higher and the chest undulation is more significant), the device produces a higher frequency and larger current outputs (as shown in Figure 4d). Whereas if using this device to monitor the deep breath, both the frequency and output current signals are much lower (dark yellow in Figure 4d). For all the cases, the current signals are synchronous to the breathing sequence, indicating that the piezoelectric sensor has a good time-resolution.

Expansion of the 2D vdWs piezoelectric materials family. Based on the above results obtained in this work, there should be a lot of other 2D vdWs piezoelectric materials, which should show similar piezoelectric properties with α-In_2Se_3 and γ-InSe. To verify this, we investigated many 2D vdWs layered materials reported in literature and studied the crystal structure collected in the database of the Crystallographic Open Database (COD).[37] We found that some vdWs layered materials with the non-centrosymmetric structures, such as ε-InSe/GaSe (*P-6m2*), γ-GaSe (*R3m*) and α-GeTe/SnTe (*R3m*), may belong to such class of piezoelectric materials.[32,38-41] The absence of inversion center in multilayer form, together with high mechanical durability, make them ideal 2D piezoelectric materials for practical application.[42]

CONCLUSIONS

In summary, we have discovered the large piezoelectric effects in a new class of 2D vdWs materials, which are ideal for flexible piezotronic/piezo-phototronic devices with both high sensitivity and good durability. The family of such vdWs layered materials has been extended. Furthermore, in addition to their correlation with piezotronics and semiconducting properties, these 2D vdWs layered materials not only expand the family of piezoelectric materials and enrich the science of 2D materials, but also enable innovative applications in flexible/wearable devices and self-powered sensors.

ASSOCIATED CONTENT

The Supporting Information is available free of charge on the ACS Publications website.

Experimental section and method, Supporting text, Figure S1-S25 and References S1-S12. (PDF)

AUTHOR INFORMATION

Corresponding Author

*hupa@hit.edu.cn

ORCID

Mingjin Dai: 0000-0001-6009-1715

Tianyou Zhai: 0000-0003-0985-4806

PingAn Hu: 0000-0003-3499-2733

Notes

The authors declare no competing financial interest.

ACKNOWLEDGMENT

This research is financially supported by the National Natural Science Foundation of China (Grant nos. 61390502, 61505033 and 61771156), the Foundation for Innovative Research Groups of the National Natural Science Foundation of China (Grant no. 51521003), the Self-Planned Task of State Key Laboratory of Robotics and System, Harbin Institute of Technology (SKLRS201607B), Engineering Physics and Science Research Council of UK (EPSRC EP/P018998/1) and Newton Mobility Grant (IE161019) through Royal Society and NSFC.

REFERENCES

(1) Fu, H. X.; Cohen, R. E., Polarization Rotation Mechanism for Ultrahigh Electromechanical Response in Single-Crystal Piezoelectrics. *Nature* **2000,** *403*, 281-283.

(2) Scott, J. F., Applications of Modern Ferroelectrics. *Science* **2007,** *315*, 954-959.

(3) Sun, E. W.; Cao, W. W., Relaxor-Based Ferroelectric Single Crystals: Growth, Domain Engineering, Characterization and Applications. *Prog. Mater. Sci.* **2014,** *65*, 124-210.

(4) Uchino, K.; Kato, K.; Tohda, M., Ultrasonic Linear Motors Using a Multilayered Piezoelectric Actuator. *Ferroelectrics* **1988,** *87*, 331-334.

(5) Panda, P. K., Review: Environmental Friendly Lead-Free Piezoelectric Materials. *Journal of Materials Science* **2009,** *44*, 5049-5062.

(6) You, Y.-M.; Liao, W.-Q.; Zhao, D.; Ye, H.-Y.; Zhang, Y.; Zhou, Q.; Niu, X.; Wang, J.; Li, P.-F.; Fu, D.-W.; Wang, Z.; Gao, S.; Yang, K.; Liu, J.-M.; Li, J.; Yan, Y.; Xiong, R.-G., An Organic-Inorganic Perovskite

Ferroelectric with Large Piezoelectric Response. *Science* **2017,** *357*, 306-309.
(7) Wu, W. Z.; Wang, L.; Li, Y. L.; Zhang, F.; Lin, L.; Niu, S. M.; Chenet, D.; Zhang, X.; Hao, Y. F.; Heinz, T. F.; Hone, J.; Wang, Z. L., Piezoelectricity of Single-Atomic-Layer MoS_2 for Energy Conversion and Piezotronics. *Nature* **2014,** *514*, 470-474.
(8) Zhu, H. Y.; Wang, Y.; Xiao, J.; Liu, M.; Xiong, S. M.; Wong, Z. J.; Ye, Z. L.; Ye, Y.; Yin, X. B.; Zhang, X., Observation of Piezoelectricity in Free-Standing Monolayer MoS_2. *Nat. Nanotechnol.* **2015,** *10*, 151-155.
(9) Duerloo, K. A. N.; Ong, M. T.; Reed, E. J., Intrinsic Piezoelectricity in Two-Dimensional Materials. *J. Phys. Chem. Lett.* **2012,** *3*, 2871-2876.
(10) Hinchet, R.; Khan, U.; Falconi, C.; Kim, S. W., Piezoelectric Properties in Two-Dimensional Materials: Simulations and Experiments. *Mater. Today* **2018,** *21*, 611-630.
(11) Blonsky, M. N.; Zhuang, H. L. L.; Singh, A. K.; Hennig, R. G., Ab Initio Prediction of Piezoelectricity in Two-Dimensional Materials. *ACS Nano* **2015,** *9*, 9885-9891.
(12) Li, W. B.; Li, J., Piezoelectricity in Two-Dimensional Group-III Monochalcogenides. *Nano Research* **2015,** *8*, 3796-3802.
(13) Wang, H.; Qian, X. F., Two-Dimensional Multiferroics in Monolayer Group IV Monochalcogenides. *2D Materials* **2017,** *4*,015042.
(14) Lee, J. H.; Park, J. Y.; Cho, E. B.; Kim, T. Y.; Han, S. A.; Kim, T. H.; Liu, Y.; Kim, S. K.; Roh, C. J.; Yoon, H. J.; Ryu, H.; Seung, W.; Lee, J. S.; Lee, J.; Kim, S. W., Reliable Piezoelectricity in Bilayer WSe_2 for Piezoelectric Nanogenerators. *Adv. Mater.* **2017,** *29*, 1606667.
(15) Bertolazzi, S.; Brivio, J.; Kis, A., Stretching and Breaking of Ultrathin MoS_2. *ACS Nano* **2011,** *5*, 9703-9709.
(16) Yang, Y. C.; Li, X.; Wen, M. R.; Hacopian, E.; Chen, W. B.; Gong, Y. J.; Zhang, J.; Li, B.; Zhou, W.; Ajayan, P. M.; Chen, Q.; Zhu, T.; Lou, J., Brittle Fracture of 2D $MoSe_2$. *Adv. Mater.* **2017,** *29*, 1604201.
(17) Xia, M.; Yin, K. B.; Capellini, G.; Niu, G.; Gong, Y. J.; Zhou, W.; Ajayan, P. M.; Xie, Y. H., Spectroscopic Signatures of AB ' and AB Stacking of Chemical Vapor Deposited Bilayer MoS_2. *ACS Nano* **2015,** *9*, 12246-12254.
(18) Jiang, T.; Liu, H. R.; Huang, D.; Zhang, S.; Li, Y. G.; Gong, X. G.; Shen, Y. R.; Liu, W. T.; Wu, S. W., Valley and Band Structure Engineering of Folded MoS_2 Bilayers. *Nat. Nanotechnol.* **2014,** *9*, 825-829.
(19) Yan, J.; Xia, J.; Wang, X.; Liu, L.; Kuo, J.-L.; Tay, B. K.; Chen, S.; Zhou, W.; Liu, Z.; Shen, Z. X., Stacking-Dependent Interlayer Coupling in Trilayer MoS_2 with Broken Inversion Symmetry. *Nano Lett.* **2015,** *15*, 8155-8161.
(20) Wang, Q. H.; Kalantar-Zadeh, K.; Kis, A.; Coleman, J. N.; Strano, M. S., Electronics and Optoelectronics of Two-Dimensional Transition Metal Dichalcogenides. *Nat. Nanotechnol.* **2012,** *7*, 699-712.
(21) Han, G.; Chen, Z. G.; Drennan, J.; Zou, J., Indium Selenides: Structural Characteristics, Synthesis and Their Thermoelectric Performances. *Small* **2014,** *10*, 2747-2765.
(22) Ding, W. J.; Zhu, J. B.; Wang, Z.; Gao, Y. F.; Xiao, D.; Gu, Y.; Zhang, Z. Y.; Zhu, W. G., Prediction of Intrinsic Two-Dimensional Ferroelectrics in In_2Se_3 and Other III_2-VI_3 van der Waals Materials. *Nat. Commun.* **2017,** *8*, 14956.
(23) Xiao, J.; Zhu, H. Y.; Wang, Y.; Feng, W.; Hu, Y. X.; Dasgupta, A.; Han, Y. M.; Wang, Y.; Muller, D. A.; Martin, L. W.; Hu, P. A.; Zhang, X., Intrinsic Two-Dimensional Ferroelectricity with Dipole Locking. *Phys. Rev. Lett.* **2018,** *120*, 227601.
(24) Zhou, Y.; Wu, D.; Zhu, Y. H.; Cho, Y. J.; He, Q.; Yang, X.; Herrera, K.; Chu, Z. D.; Han, Y.; Downer, M. C.; Peng, H. L.; Lai, K. J., Out-of-Plane Piezoelectricity and Ferroelectricity in Layered Alpha-In_2Se_3 Nanoflakes. *Nano Lett.* **2017,** *17*, 5508-5513.
(25) Xue, F.; Hu, W. J.; Lee, K. C.; Lu, L. S.; Zhang, J. W.; Tang, H. L.; Han, A.; Hsu, W. T.; Tu, S. B.; Chang, W. H.; Lien, C. H.; He, J. H.; Zhang, Z. D.; Li, L. J.; Zhang, X. X., Room-Temperature Ferroelectricity in Hexagonally Layered Alpha-In_2Se_3 Nanoflakes Down to the Monolayer Limit. *Adv. Funct. Mater.* **2018,** *28*, 1803738.
(26) Michel, K. H.; Verberck, B., Theory of Phonon Dispersions and Piezoelectricity in Multilayers of Hexagonal Boron-Nitride. *Phys. Status Solidi B* **2011,** *248*, 2720-2723.
(27) Wuzhang Fang, L.-C. Z., Guangzhao Qin, Qing-Bo Yan, Qing-Rong Zheng,; Su, G., Layer Dependence of Geometric, Electronic and Piezoelectric Properties of SnSe. *https://arxiv.org/abs/1603.01791* **2016**.
(28) Li, Y. L.; Rao, Y.; Mak, K. F.; You, Y. M.; Wang, S. Y.; Dean, C. R.; Heinz, T. F., Probing Symmetry Properties of Few-Layer MoS_2 and h-BN by Optical Second-Harmonic Generation. *Nano Lett.* **2013,** *13*, 3329-3333.
(29) Zhou, X.; Cheng, J. X.; Zhou, Y. B.; Cao, T.; Hong, H.; Liao, Z. M.; Wu, S. W.; Peng, H. L.; Liu, K. H.; Yu, D. P., Strong Second-Harmonic Generation in Atomic Layered GaSe. *J. Am. Chem. Soc.* **2015,** *137*, 7994-7997.
(30) Wells, S. A.; Henning, A.; Gish, J. T.; Sangwan, V. K.; Lauhon, L. J.; Hersam, M. C., Suppressing Ambient Degradation of Exfoliated Inse Nanosheet Devices Via Seeded Atomic Layer Deposition Encapsulation. *Nano Lett.* **2018**, *18*, 7876-7882.
(31) Wang, Z. L.; Song, J. H., Piezoelectric Nanogenerators Based on Zinc Oxide Nanowire Arrays. *Science* **2006,** *312*, 242-246.

(32) Hao, Q.; Yi, H.; Su, H.; Wei, B.; Wang, Z.; Lao, Z.; Chai, Y.; Wang, Z.; Jin, C.; Dai, J.; Zhang, W., Phase Identification and Strong Second Harmonic Generation in Pure ε-InSe and Its Alloys. *Nano Lett.* **2019,** *19*, 2634-2640.
(33) Yang, Z. B.; Jie, W. J.; Mak, C. H.; Lin, S. H.; Lin, H. H.; Yang, X. F.; Yan, F.; Lau, S. P.; Hao, J. H., Wafer-Scale Synthesis of High-Quality Semiconducting Two-Dimensional Layered InSe with Broadband Photoresponse. *ACS Nano* **2017,** *11*, 4225-4236.
(34) Dai, M. J.; Chen, H. Y.; Feng, R.; Feng, W.; Hu, Y. X.; Yang, H. H.; Liu, G. B.; Chen, X. S.; Zhang, J.; Xu, C. Y.; Hu, P. A., A Dual-Band Multilayer Inse Self-Powered Photodetector with High Performance Induced by Surface Plasmon Resonance and Asymmetric Schottky Junction. *ACS Nano* **2018**, *12*, 8739-8747.
(35) Dai, M.; Chen, H.; Wang, F.; Hu, Y.; Wei, S.; Zhang, J.; Wang, Z.; Zhai, T.; Hu, P., Robust Piezo-Phototronic Effect in Multilayer γ-Inse for High-Performance Self-Powered Flexible Photodetectors. *ACS Nano* **2019**, *13*, 7291-7299.
(36) Schwartz, G.; Tee, B. C. K.; Mei, J. G.; Appleton, A. L.; Kim, D. H.; Wang, H. L.; Bao, Z. N., Flexible Polymer Transistors with High Pressure Sensitivity for Application in Electronic Skin and Health Monitoring. *Nat. Commun.* **2013,** *4*, 1859.
(37) Gražulis, S.; Daškevič, A.; Merkys, A.; Chateigner, D.; Lutterotti, L.; Quirós, M.; Serebryanaya, N. R.; Moeck, P.; Downs, R. T.; Le Bail, A., Crystallography Open Database (COD): An Open-Access Collection of Crystal Structures and Platform for World-Wide Collaboration. *Nucleic Acids Res.* **2012,** *40*, D420-D427.
(38) Chang, K.; Liu, J. W.; Lin, H. C.; Wang, N.; Zhao, K.; Zhang, A. M.; Jin, F.; Zhong, Y.; Hu, X. P.; Duan, W. H.; Zhang, Q. M.; Fu, L.; Xue, Q. K.; Chen, X.; Ji, S. H., Discovery of Robust in-Plane Ferroelectricity in Atomic-Thick SnTe. *Science* **2016,** *353*, 274-278.
(39) Plekhanov, E.; Barone, P.; Di Sante, D.; Picozzi, S., Engineering Relativistic Effects in Ferroelectric SnTe. *Phys. Rev. B* **2014,** *90*, 161108.
(40)Li, X. F.; Basile, L.; Yoon, M.; Ma, C.; Puretzky, A. A.; Lee, J.; Idrobo, J. C.; Chi, M. F.; Rouleau, C. M.; Geohegan, D. B.; Xiao, K., Revealing the Preferred Interlayer Orientations and Stackings of Two-Dimensional Bilayer Gallium Selenide Crystals. *Angew. Chem., Int. Ed.* **2015,** *54*, 2712-2717.
(41) Rinaldi, C.; Varotto, S.; Asa, M.; Slawinska, J.; Fujii, J.; Vinai, G.; Cecchi, S.; Di Sante, D.; Calarco, R.; Vobornik, I.; Panaccione, G.; Picozzi, S.; Bertacco, R., Ferroelectric Control of the Spin Texture in GeTe. *Nano Lett.* **2018,** *18*, 2751-2758.
(42) Wu, W. Z.; Wang, Z. L., Piezotronics and Piezo-Phototronics for Adaptive Electronics and Optoelectronics. *Nat. Rev. Mater.* **2016,** *1*, 6031.

ToC:

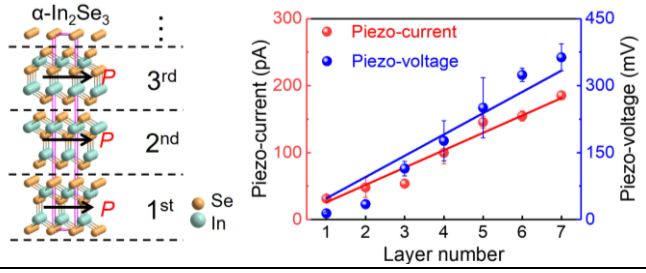
α-In2Se3
P
3rd
2nd
1st
Se
In
Piezo-current
Piezo-voltage
Piezo-current (pA)
Piezo-voltage (mV)
Layer number
0
100
200
300
150
300
450
1
2
3
4
5
6
7